THE JOURNAL OF PHYSICAL CHEMISTRY Letters

Letter

pubs.acs.org/JPCL

A Comparison of Charge Separation Dynamics in Organic Blend Films Employing Fullerene and Perylene Diimide Electron Acceptors

Safa Shoaee,*[,†,∥] Florent Deledalle,[†] Pabitra Shakya Tuladhar,[†] Ravichandran Shivanna,[‡] Sridhar Rajaram,[§] K. S. Narayan,[‡] and James R. Durrant*[,†]

[†]Centre for Plastic Electronics, Department of Chemistry, Imperial College London, London SW7 2AZ, United Kingdom

[‡]Chemistry and Physics of Materials Unit, Jawaharlal Nehru Centre for Advanced Scientific Research, Bangalore 560064, India

[§]International Centre for Materials Science, Jawaharlal Nehru Centre for Advanced Scientific Research, Bangalore 560064, India

Supporting Information

ABSTRACT: We report a comparison of charge carrier dynamics and device performance for low band gap polymer PBDTTT-CT in blends with the fullerene acceptor $PC_{71}BM$ and a PDI derivative with similar electron affinities. Charge separation and recombination dynamics are found to be remarkably similar for these two acceptors, with both blends exhibiting efficient, ultrafast charge separation (time constants of 1.6 and 1.4 ps, respectively). The lower device performance for the PDI acceptor (1.75% compared to 3.5% for the equivalent $PC_{71}BM$ device) is shown to result from slower charge transport, increasing nongeminate recombination losses during charge collection.

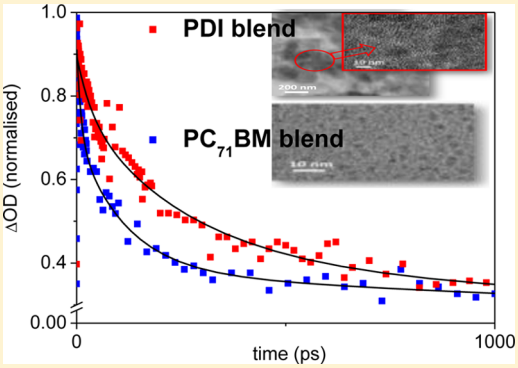

Solution processed, bulk heterojunction organic solar cells (OSC) are attracting significant attention due to their potential for low-cost and scalable solar energy conversion. Such devices are typically based on blend films of a polymer electron donor and a small molecule electron acceptor. To date, most successful electron acceptors used in these devices are based on fullerene derivatives, including in particular [6,6]-phenyl-C71-butyric acid methyl ester ($PC_{71}BM$). However, the challenging synthesis and high cost of fullerene derivatives and their relatively weak light absorption limit their suitability for commercial application.[1,2] There is therefore significant interest in the development of alternative nonfullerene electron acceptors. Several classes of solution-processable nonfullerene molecular acceptors have been considered to date[3−6] with, for example, recent reports of device efficiencies over 4% with perylene diimide acceptors.[7,8] Such advances in device efficiencies with nonfullerene acceptors have primarily resulted from materials design strategies to improve blend nanomorphology.[8,9] However, despite these advances, the attainment of solution processed organic solar cells employing nonfullerene electron acceptors with comparable efficiencies to $PC_{71}BM$ remains a significant, and to date unfulfilled, challenge for the technological development of organic solar cells.

Several factors have been identified as enabling the high efficiencies of OSC's employing PCBM as an electron acceptor. These include its structural, optical, charge delocalization, charge transport, and energetic properties. Most studies to date addressing the function and optimization of nonfullerene acceptors in OSC have focused upon blend nanomorphology and its impact in particular upon charge collection efficiency.[10,11] An additional consideration is the efficiency and kinetics of charge separation. Several recent studies have focused upon the favorable properties of PCBM with regard to charge separation, including, for example, the potential for $PC_{71}BM$'s electron acceptor orbitals to be delocalized over several neighboring fullerenes, thereby facilitating ultrafast electron motion away from the donor/acceptor interface.[12,13] However, direct comparison of charge separation dynamics between fullerene and nonfullerene acceptors have been relatively limited to date.[14,15] For example, it has been suggested by Asbury et al. that when blended with the crystalline donor polymer P3HT charge separation to PDI electron acceptors is thermally activated, whereas that of $PC_{60}BM$ is not.[16] Other studies have reported ultrafast charge separation dynamics for polymer/PDI blend films and that charge dissociation in such blend films may, for some donor polymers, be less sensitive to the energetic offset driving charge separation.[17]

In this paper we focus upon a comparison of charge carrier dynamics of blend films of the donor polymer poly[(4,8-bis[5-(2-ethylhexyl)thiophene-2-yl]benzo[1,2-b:4,5-b′]dithiophene)-2,6-diyl-*alt*-(4-(2-ethylhexanoyl)-thieno[3,4-*b*]thiophene))-2,6-diyl] (PBDTTT-CT) with $PC_{71}BM$ and a soluble PDI acceptors. The structures of these molecules are shown in

Received: November 10, 2014
Accepted: December 17, 2014
Published: December 17, 2014

DOI: 10.1021/jz502385n
J. Phys. Chem. Lett. 2015, 6, 201−205

Supporting Information Scheme S1, as well as their energetics. This PDI was selected as it exhibits a similar electron affinity to $PC_{71}BM$, thus allowing us to compare charge dynamics in blend films with different molecular acceptors but similar energy offsets driving charge separation. PBDTTT-CT is an amorphous, low bandgap donor polymer, which has been shown to exhibit promising device efficiencies with both $PC_{71}BM$[18] and PDI[8,17,19] electron acceptors. Near infrared (NIR) transient absorption spectroscopy (TAS) covering time scales from 200 fs−6 ns is employed to monitor the kinetics and efficiency of charge carrier generation in blend films. These transient optical studies are complimented by transient optoelectronic studies of charge collection and nongeminate recombination and device current/voltage analysis in order to elucidate the factors determining the differences in device efficiency between these PDI and $PC_{71}BM$ acceptors.

Absorption and emission spectra of the pristine materials and blend films are presented in Figure 1. For both acceptors, 1:1

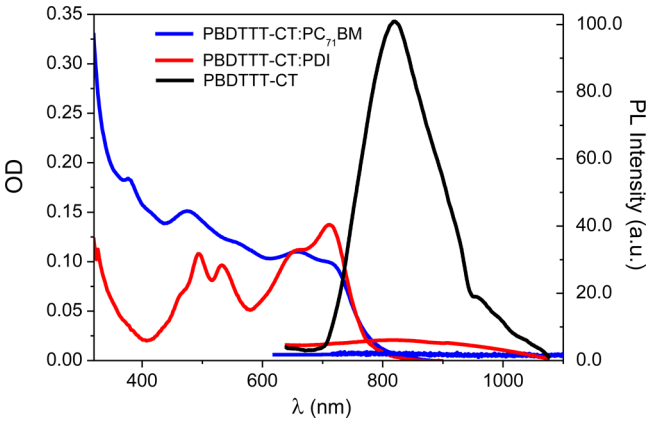

Figure 1. Ground state absorption spectra of PBDTTT-CT:PDI (1:1, red) and PBDTTT-CT:$PC_{71}BM$ (1:1, blue) blend films and their corresponding photoluminescence spectra, as well as a PBDTTT-CT control (black).

blend films were employed. For the photoluminescence data, an excitation wavelength of 632 nm was employed to achieve selective optical excitation of the low bandgap donor polymer. In both blend films, PBDTTT-CT photoluminescence was strongly quenched relative to the neat polymer film, by 99% in the blend with PCBM and 90% in the blend with PDI. The slightly lower PL quenching with the PDI acceptor is attributed to the higher tendency of this PDI to crystallize compared to $PC_{71}BM$, resulting in less mixing of the donor and acceptor species, as evidenced by both high resolution transmission electron diffraction and X-ray diffraction data (see Supporting Information).[20] Nevertheless, the strong polymer emission quenching in both blend films is clearly indicative of mixing of polymer and acceptor species on length scales much less than the polymer exciton diffusion length and indicates efficient polymer exciton separation in both blends.

We turn now to the kinetics of charge separation and recombination in these blend films, as measured using transient absorption spectroscopy, using 700 nm excitation wavelength to ensure selective excitation of the donor polymer. Figure 2 shows typical NIR transient absorption spectra of neat PBDTTT-CT, PBDTTT-CT:PDI, and PBDTTT-CT:$PC_{71}BM$ blend films on picosecond−nanosecond time scales, with the corresponding kinetics at a two probe wavelengths (1420 and

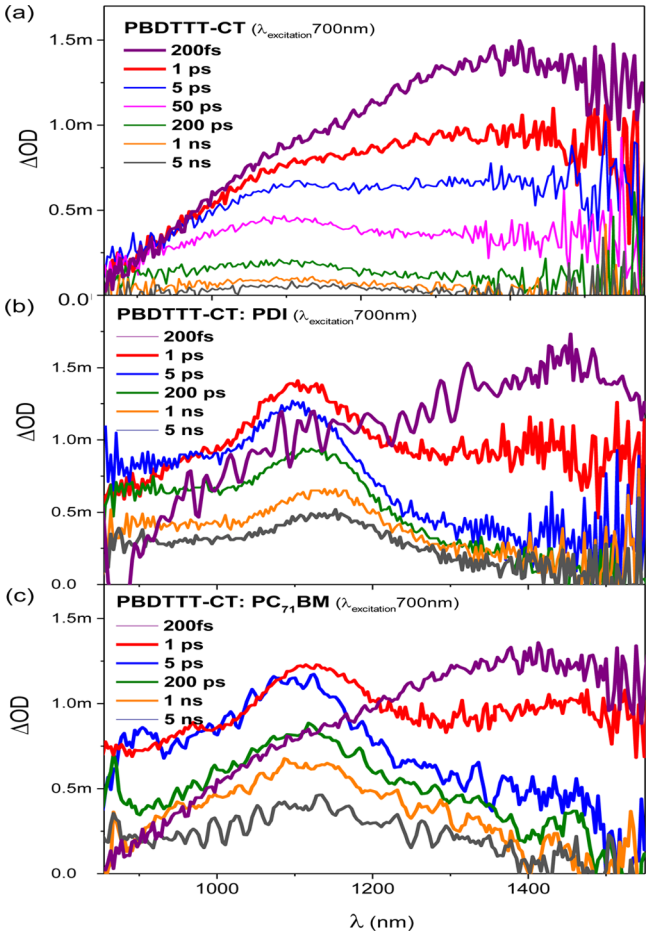

Figure 2. Femtosecond transient absorption spectra of (a) neat PBDTTT-CT, (b) blend of PBDTTT-CT:PDI (1:1), and (c) blend of PBDTTT-CT:$PC_{71}BM$ (1:1), all excited at 700 nm. Neat film excited with an intensity of 3 μJ cm^{-2} and blends films excited at 1 μJ cm^{-2}.

1100 nm) being shown in Figure 3. The NIR transient absorption for the neat PBDTTT-CT has been assigned previously to photoinduced absorption from singlet excitons, peaking at 1420 nm.[9] A small residual shoulder at ≈1100 nm is increasingly apparent at long times (>50 ps) and assigned to a low yield of long-lived polarons/triplet states.

For both blend films, the transient absorption spectra at early times (200 fs) exhibit a broad absorption peaking at ≈1420 nm similar to that of the neat film. However, for these blend films, this spectrum rapidly evolves to a narrower photoinduced absorption peaking at 1100 nm. This spectral evolution is analogous to that we have reported previously for blends of PBDTTT-CT with an amorphous PDI dimer.[9] As previously, it is assigned to photoinduced charge separation from polymer singlet excitons to polarons. The striking similarity between the spectra observed for both the PBDTTT-CT:$PC_{71}BM$ and PBDTTT-CT:PDI blend films confirms the photoinduced absorption over this spectral range is dominated by polymer exciton and polaron absorption.

Figure 3a compares the PBDTTT-CT exciton decay dynamics for the two blend films, monitored at the PBDTTT-CT exciton photoinduced absorption maximum of 1420 nm. In both cases, the decay dynamics are dominated by a monoexponential decay phase assigned to photoinduced charge separation, with the small residual signal being assigned to polaron absorption. It is apparent that both blends exhibit

DOI: 10.1021/jz502385n
J. Phys. Chem. Lett. 2015, 6, 201−205

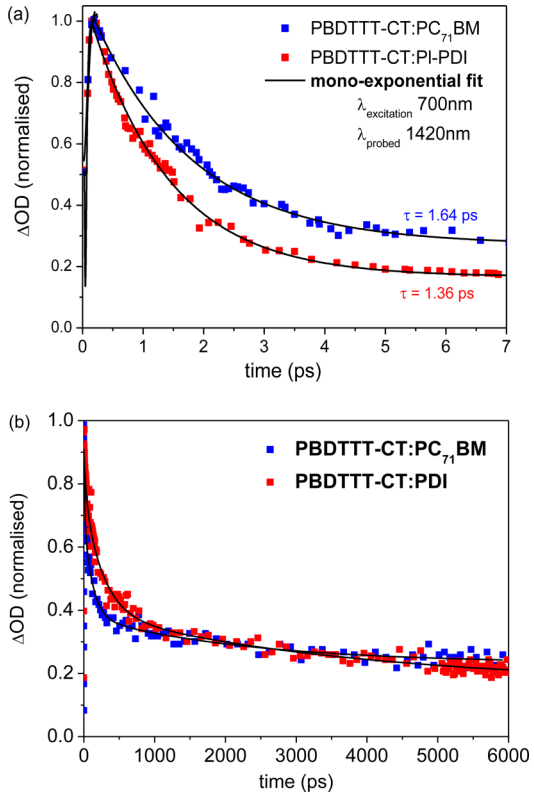

Figure 3. Femtosecond transient absorption decays dynamics of PBDTTT-CT:PDI (1:1, red) and PBDTTT-CT:$PC_{71}BM$ (1:1, blue) blend films excited at 700 nm probed at (a) 1420 nm and (b) 1100 nm. The solid lines represent monoexponential (a) and power law (b) fits to the data.

similar decay dynamics, with decay time constants of 1.4 ± 0.2 ps for the PBDTTT-CT:PDI blend and 1.6 ± 0.2 ps for the PBDTTT-CT:$PC_{71}BM$ blend. Thus, it is apparent that for these two blends employing acceptors with very different molecular structures but similar energetics, the kinetics of charge separation are very similar.

The decay dynamics of the PBDTTT-CT polaron absorption at 1100 nm are plotted for the two blend films in Figure 3b. At early times (<2 ps), a rise is observed in this absorption is assigned to photoinduced charge separation. At longer times, both blend films show approximately a power law, decay of this polaron absorption extending to beyond the measurement time scale (0−6 ns), assigned to polaron recombination to ground. These dynamics are intensity dependent, accelerating as the excitation density is increased (see Figure S3, Supporting Information), indicating they should be assigned to non-geminate recombination of dissociated polarons rather than bound polaron pairs. At the lowest excitation density employed (1 μJ cm^{-2}), the decay dynamics are rather similar (decay half-times of ≈250 and 500 ps with $PC_{71}BM$ and PDI, respectively), indicative of similar, rather fast, nongeminate recombination dynamics for the blend films employing the two electron acceptors.

Our observation of similar charge separation and recombination dynamics for the for the PBDTTT-CT:$PC_{71}BM$ and PBDTTT-CT:PDI blend films of course does not imply that in general these dynamics are independent of acceptor molecular structure. Rather it only demonstrates that there in terms of these dynamics, PCBM is not unique, in that a PDI acceptor with similar energetics can yield similar dynamics. For example, we have previously reported that the dependence of geminate recombination losses upon donor/acceptor energetics is different for blends with PCBM and PDI's.[14,15] The dynamics are also expected to be dependent upon film nanomorphology. Our observation of similar dynamics suggests that although the PDI employed shows somewhat higher crystallinity than $PC_{71}BM$ in the blend, this difference is not enough to change substantially the kinetics of exciton separation and nongeminate recombination.

We thus conclude that for the PBDTTT-CT:$PC_{71}BM$ and PBDTTT-CT:PDI blend films studied herein, the kinetics of charge separation and recombination monitored in blend films are remarkably similar. We turn now to the function of these blend films in photovoltaic devices. A series of photovoltaic devices employing inverted device architectures—ITO/ZnO/active layer/MoO_3/Ag—were fabricated, consisting of PBDTTT-CT as donor polymer and either PDI or $PC_{71}BM$ as acceptor in 1:1 blends. Full device fabrication details are given in the experimental section. Devices employing PDI as acceptor showed optimum device efficiencies for rather thin photoactive layers (40 nm), with both fill factor and short circuit current decreasing with increased device thickness. Figure 4a shows current/voltage data for devices with each acceptor, employing 40 and 50 nm thick photoactive layers for PDI and $PC_{71}BM$ acceptors, respectively. It is apparent the performance of the PBDTTT-CT:PDI device is limited primarily by a relatively low fill factor, as well as lower short circuit current, resulting in a device efficiency of 1.7% compared to 3.5% for the equivalent thickness device employing $PC_{71}BM$.

The lower fill factor, and strong thickness dependence, of the photovoltaic performance of the PBDTTT-CT:PDI devices is strongly indicative of charge carrier collection losses limiting performance. This conclusion is strongly supported by the light intensity analysis of J_{SC} (Figure 4b), which shows that the PBDTTT-CT:PDI exhibits strongly nonlinear behavior ($J_{SC} \propto LI^{\alpha}$ with α = 0.4 for PDI as acceptor and 0.7 for PCBM as acceptor). This nonlinear behavior is consistent with charge collection losses due to nongeminate recombination during transport limiting FF and J_{SC} with PDI as acceptor. Transient photovoltage studies of charge carrier lifetimes measured at open circuit (Figure 4c) showed very similar carrier lifetimes for both acceptors, indicative of similar nongeminate recombination for both devices and consistent with our transient absorption data above (Figure 3b). This suggests that the poor collection efficiencies exhibited by the PBDTTT-CT:PDI devices do not derive from faster recombination losses but rather from slower charge transport. Support for this conclusion comes from comparison of charge extraction transients for these two devices, measured at short circuit following stepped one sun irradiation (Figure 4d). It is apparent that the charge extraction transient for the PBDTTT-CT:PDI device is at least an order of magnitude slower than the PBDTTT-CT:$PC_{71}BM$ device, and extends out to tens of microseconds time scales. Bias dependent transient absorption data (Supporting Information Figure S5) suggests that field-dependent geminate losses are relatively insignificant for the devices studied herein (the observation of field dependent losses by Gehrig et al.[21] for a similar material system may be related to differences in material crystallinity). Although it is not possible to use the data reported herein to make a quantitative analysis of nongeminate recombination losses during charge collection, it is apparent that the charge extraction kinetics for the PBDTTT-CT:PDI device are on a

DOI: 10.1021/jz502385n
J. Phys. Chem. Lett. 2015, 6, 201−205

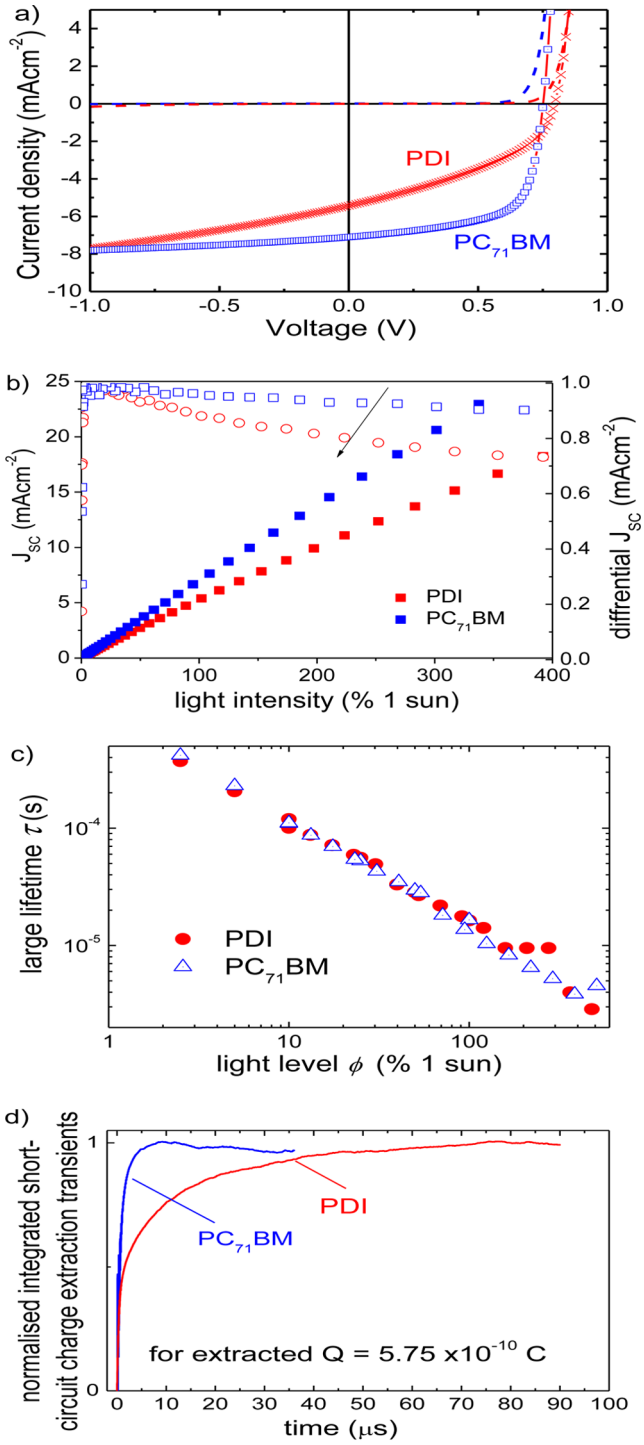

Figure 4. (a) AM 1.5 current−voltage response of PBDTTT-CT:PDI (red) and PBDTTT-CT:$PC_{71}BM$ (blue). (b) Short-circuit current densities (left axis, solid symbols) and their relative normalized derivative (right axis, open symbols) with light intensity Φ for PBDTTT-CT:PDI and PBDTTT-CT:$PC_{71}BM$. (c) TPV small perturbation lifetime $\tau_{\Delta n}$ at different illumination level Φ for PBDTTT-CT:PDI and PBDTTT-CT:$PC_{71}BM$. (d) Charge extraction transient through 50 Ohms resistance at short-circuit under 1 sun illumination level for PBDTTT-CT:PDI and PBDTTT-CT:$PC_{71}BM$.

similar time scale to the nongeminate charge losses measured by the TPV transients ($\tau \sim 10$ μs at one sun), consistent with such losses significantly impacting upon device performance.

We note the nongeminate recombination lifetimes in PBDTTT-CT:$PC_{71}BM$ blend films obtained by our TPV analyses (microseconds) are substantially slower than those films obtained from our transient absorption studies (picoseconds). This contrasts to our studies of P3HT:PCBM blend films, where under appropriate conditions, similar time constants were obtained for both techniques.[22] This can be understood as resulting from the relative slow (non-Langevin) recombination observed for P3HT:$PC_{71}BM$, resulting in substantial charge accumulation in such devices under the open circuit conditions employed for TPV measurements, similar to the charge densities generated under the pulsed laser excitation employed in transient absorption studies (typically 1−10 μJ cm^{-2}). For PBDTTT-CT blends, nongeminate recombination is substantially faster, resulting in much less charge accumulation at open circuit, such that the transient absorption measurements are undertaken at charge densities substantially greater than those obtained under operating conditions. Nevertheless, both measurements allow relative comparison of nongeminate recombination losses between equivalent blends with different electron acceptors, as employed herein. We note that these nongeminate recombination losses are also likely to be composition dependent, a consideration beyond the scope of the study reported herein.

In summary, we have compared charge separation and recombination dynamics as well as device performance for organic solar cells employing the donor polymer PBDTTT-CT blended with two electron acceptors, a PDI derivative and $PC_{71}BM$, selected for their similar electron affinities. The lower device performance of the PBDTTT-CT:PDI is shown to be due primarily to less efficient charge collection due to slower charge transport. This conclusion is consistent with previous nanomorphology studies and our own structural data (see Supporting Information), which indicate that the performance of polymer:PDI solar cells is primarily limited by poor transport in blend due to unfavorable blend microstructure. In contrast, we find that the charge separation and nongeminate recombination dynamics of these two blend films are strikingly similar. As such, we find that $PC_{71}BM$ does not exhibit particularly favorable properties as an electron acceptor relative to PDI in terms of its primary function of enabling charge separation across a donor/acceptor interface. These conclusions further emphasize the potential for nonfullerene acceptors to function in efficient organic solar cells.

■ ASSOCIATED CONTENT

Ⓢ Supporting Information

Supporting Information on experimental section and schematics and further figures on cyclic voltammetry, XRD, TEM and transient absorption decay dynamics and transient photovoltage of the two systems are available. This material is available free of charge via the Internet at http://pubs.acs.org.

■ AUTHOR INFORMATION

Corresponding Authors

*E-mail: s.shoaee06@imperial.ac.uk.
*E-mail: j.durrant@imperial.ac.uk.

Present Address

‖Centre for Organic Photonics & Electronics, The University of Queensland, Brisbane, Queensland 4072, Australia.

Notes

The authors declare no competing financial interest.

DOI: 10.1021/jz502385n
J. Phys. Chem. Lett. 2015, 6, 201−205

■ ACKNOWLEDGMENTS

We thank the EPSRC projects APEX EP/H040218/1 and EP/G031088/1 for financial support.

■ REFERENCES

(1) Nielsen, T. D.; Cruickshank, C.; Foged, S.; Thorsen, J.; Krebs, F. C. Business, Market and Intellectual Property Analysis of Polymer Solar Cells. *Sol. Energy Mater. Sol. Cells* **2010**, *94*, 1553−1571.

(2) Anctil, A.; Babbitt, C. W.; Raffaelle, R. P.; Landi, B. J. Material and Energy Intensity of Fullerene Production. *Environ. Sci. Technol.* **2011**, *45*, 2353−2359.

(3) Lin, Y.; Li, Y.; Zhan, X. A Solution-Processable Electron Acceptor Based on Dibenzosilole and Diketopyrrolopyrrole for Organic Solar Cells. *Adv. Energy Mater.* **2013**, *3*, 724−728.

(4) Zhou, Y.; Dai, Y.-Z.; Zheng, Y.-Q.; Wang, X.-Y.; Wang, J.-Y.; Pei, J. Non-Fullerene Acceptors Containing Fluoranthene-Fused Imides for Solution-Processed Inverted Organic Solar Cells. *Chem. Commun.* **2013**, *49*, 5802−5804.

(5) Bloking, J. T.; Han, X.; Higgs, A. T.; Kastrop, J. P.; Pandey, L.; Norton, J. E.; Risko, C.; Chen, C. E.; Bredas, J.-L.; McGehee, M. D.; et al. A. Solution-Processed Organic Solar Cells with Power Conversion Efficiencies of 2.5% using Benzothiadiazole/Imide-Based Acceptors. *Chem. Mater.* **2011**, *23*, 5484−5490.

(6) Verreet, B.; Rand, B. P.; Cheyns, D.; Hadipour, A.; Aernouts, T.; Heremans, P.; Medina, A.; Claessens, C. G.; Torres, T. A 4% Efficient Organic Solar Cell Using a Fluorinated Fused Subphthalocyanine Dimer as an Electron Acceptor. *Adv. Energy Mater.* **2011**, *1*, 565−568.

(7) Lu, Z.; Jiang, B.; Zhang, X.; Tang, A.; Chen, L.; Zhan, C.; Yao, J. Perylene-Diimide Based Non-Fullerene Solar Cells with 4.34% Efficiency through Engineering Surface Donor/Acceptor Compositions. *Chem. Mater.* **2014**, *26*, 2907−2914.

(8) Zhang, X.; Lu, Z.; Ye, L.; Zhan, C.; Hou, J.; Zhang, S.; Jiang, B.; Zhao, Y.; Huang, J.; Zhang, S.; et al. A Potential Perylene Diimide Dimer-Based Acceptor Material for Highly Efficient Solution-Processed Non-Fullerene Organic Solar Cells with 4.03% Efficiency. *Adv. Mater.* **2013**, *25*, 5791−5797.

(9) Shivanna, R.; Shoaee, S.; Dimitrov, S.; Kandappa, S. K.; Rajaram, S.; Durrant, J. R.; Narayan, K. Charge Generation and Transport in Efficient Organic Bulk Heterojunction Solar Cells with a Perylene Acceptor. *Energy Environ. Sci.* **2014**, *7*, 435−441.

(10) Sharenko, A.; Proctor, C. M.; van der Poll, T. S.; Henson, Z. B.; Thuc-Quyen, N.; Bazan, G. C. A High-Performing Solution-Processed Small Molecule: Perylene Diimide Bulk Heterojunction Solar Cell. *Adv. Mater.* **2013**, *25*, 4403−4406.

(11) Savoiea, B. M.; Kohlstedta, K. L. K.; Jacksona, N. E.; Chena, L. X.; de la Cruza, M. O.; Schatza, G. C.; Marksa, T. J.; Ratnera, M. A. Mesoscale Molecular Network Formation in Amorphous Organic Materials. *Proc. Natl. Acad. Sci. U.S.A.* **2014**, *111*, 10055−10060.

(12) Bakulin, A. A.; Rao, A.; Pavelyev, V. G.; van Loosdrecht, P. H. M.; Pshenichnikov, M. S.; Niedzialek, D.; Cornil, J.; Beljonne, D.; Friend, R. H. The Role of Driving Energy and Delocalized States for Charge Separation in Organic Semiconductors. *Science* **2012**, *335*, 1340−1344.

(13) Poelking, C.; Daoulas, K.; Troisi, A.; Andrienko, D. Morphology and Charge Transport in P3HT: A Theorist's Perspective. *Adv. Polym. Sci.* **2014**, *265*, 139−180.

(14) Shoaee, S.; An, Z.; Zhang, X.; Barlow, S.; Marder, S. R.; Duffy, W.; Heeney, M.; McCulloch, I.; Durrant, J. R. Charge Photogeneration in Polythiophene/Perylene Diimide Films. *Chem. Commun.* **2009**, 5445 −5447.

(15) Shoaee, S.; Clarke, T. M.; Huang, C.; Barlow, S.; Marder, S. R.; Heeney, M.; McCulloch, I.; Durrant, J. R. Acceptor Energy Level Control of Charge Photogeneration in Organic Donor/Acceptor Blends. *J. Am. Chem. Soc.* **2010**, *132*, 12919−12926.

(16) Pensack, R. D.; Guo, C.; Vakhshouri, K.; Gomez, E. D.; Asbury, J. B. Influence of Acceptor Structure on Barriers to Charge Separation in Organic Photovoltaic Materials. *J. Phys. Chem. C* **2012**, *116*, 4824−4831.

(17) Rajaram, S.; Shivanna, R.; Kandappa, S. K.; Narayan, K. S. Nonplanar Perylene Diimides as Potential Alternatives to Fullerenes in Organic Solar Cells. *J. Phys. Chem. Lett.* **2012**, *3*, 2405−2408.

(18) Fan, X.; Fang, G.; Cheng, F.; Qin, P.; Huang, H.; Li, Y. Enhanced Performance and Stability in PBDTTT-C-T: PC70 BM Polymer Solar Cells by Optimizing Thickness of NiO_x Buffer Layers. *J. Phys. D: Appl. Phys.* **2013**, 46.

(19) Singh, R.; Aluicio-Sarduy, E.; Kan, Z.; Ye, T.; MacKenzie, R. C. I.; Keivanidis, P. E. Fullerene-Free Organic Solar Cells with an Efficiency of 3.7% Based On a Low-Cost Geometrically Planar Perylene Diimide Monomer. *Journal of Materials Chemistry A* **2014**, *2*, 14348−14353.

(20) Shoaee, S.; Subramaniyan, S.; Xin, H.; Keiderling, C.; Tuladhar, P. S.; Jamieson, F.; Jenekhe, S. A.; Durrant, J. R. Charge Photogeneration for a Series of Thiazolo-Thiazole Donor Polymers Blended with the Fullerene Electron Acceptors PCBM and ICBA. *Adv. Funct. Mater.* **2013**, *23*, 3286−3298.

(21) Gehrig, D.; Howard, I. A.; Kamm, V.; Dyer-Smith, C.; Etzold, F.; Laquai, F. Charge Generation in Polymer: Perylene Diimide Blends Probed by Vis-NIR Broadband Transient Absorption Pump−Probe Spectroscopy. *Phys. Chem. Interfaces Nanomater. XII* **2013**, *8811*.

(22) Shuttle, C. G.; Regan, B. O.; Ballantyne, A. M.; Nelson, J.; Bradley, D. D. C.; Durrant, J. R. Bimolecular recombination losses in polythiophene: Fullerene solar cells. *Phys. Rev. B: Condens. Matter Mater. Phys.* **2008**, *78*, 113201.

DOI: 10.1021/jz502385n
J. Phys. Chem. Lett. 2015, 6, 201−205